163
1-25-83
I-7524
Dr. 1136

LA-9632-PR

Progress Report

Los Alamos National Laboratory is operated by the University of California for the United States Department of Energy under contract W-7405-ENG-36.

Flight-Systems Safety Program

August 1982

Los Alamos
Los Alamos National Laboratory
Los Alamos, New Mexico 87545

DISCLAIMER

The four most recent reports in this series, unclassified, are LA-9476-PR, LA-9547-PR, LA-9548-PR, and LA-9550-PR.

This work was supported by the US Department of Energy, Office of Special Nuclear Projects.

Photocomposition by E. Katherine Valdez

LA-9632-PR
Progress Report

UC-33a
Issued: December 1982

LA--9632-PR

DE83 005608

Flight-Systems Safety Program

August 1982

Compiled by
S. E. Bronisz

Los Alamos National Laboratory
Los Alamos, New Mexico 87545

FLIGHT SYSTEMS SAFETY PROGRAM
August 1982

Compiled by
S. E. Bronisz

ABSTRACT

This technical monthly report covers studies related to the use of $^{238}PuO_2$ in radioisotope power systems carried out for the Office of Special Nuclear Projects of the US Department of Energy by Los Alamos National Laboratory. Most of the studies discussed here are ongoing. Results and conclusions described may change as the work continues.

I. GENERAL-PURPOSE HEAT SOURCE

A. Impact Test Results (F. W. Schonfeld)

The metallographic examinations of the welds and cup walls of the clads used in the third design iteration test (DIT-3) of a General-Purpose Heat Source (GPHS) module were completed. The DIT-3 test was designed to determine the effect of weld defect size on the impact response of a GPHS module that is impacted with the impact assembly axes tilted 30° to the target surface. As reported last month,[1] none of the clads failed; the overall deformations were similar to those seen after prior tests at the 0° orientation, but the local strains were different.

After the external photography and examinations, the four capsules were cut open, defueled, and examined, and samples were removed for microscopic examination.

Fig. 1. The internal surface of the weld overlap region of capsule SRP-127 had surface defects, but no cracks were visible (12X).

1. Fueled Clad SRP-127. This fueled clad was in the trailing position (closure end) of impact shell TGL-11. It had an ultrasonic defect indication of 9.0 (arbitrary units). Figure 1 shows the internal surface at the point of weld submergence. Some apparent surface defects are visible in the weld overlap region ahead of the submergence point, but no cracks like those expected for the defect level can be seen.

The as-polished and etched microstructures of the weld overlap are shown in Fig. 2. Some small surface defects and a very small amount of grain-boundary porosity are visible. A rough area below the largest surface crack was visible after etching (Fig. 2b). It may be an internal defect that affected the ultrasonic signal.

A cross section of the single-pass weld region is shown in Fig. 3. Again, a few surface cracks are visible, along with some internal porosity. It is not possible to know whether the defects seen were created by the impact or merely expanded by it. In general, the weld structure is very acceptable, with many grains along the centerline and no pronounced direct path through them.

Typical microstructures of the walls of capsule SRP-127 are shown in Fig. 4. The grains are not equiaxed but are somewhat elongated, with the vent cup (Fig. 4a) possessing this characteristic somewhat more than the shield cup does (Fig. 4b). The transverse grain counts of the cups that made up SRP-127 are listed in Table I.

An atypical microstructure observed in capsule SRP-127 is shown in Fig. 5. These large grains were found on the outside of the radius on the vent cup. They are localized, and their presence suggests that secondary recrystallization can occur under some conditions.

2. Fueled Clad SRP-140. This fueled clad was in the trailing position (solid end) of impact assembly TGL-2. It had an ultrasonic defect indication of 11.5, the largest of the capsules in DIT-3. Figure 6 shows the internal surface in the area of weld submergence. Several small cracks can be seen just beyond the point of submergence. Again, the cracks appear to be too small to cause the 11.5 ultrasonic level. A partial explanation of the apparent discrepancy between the ultrasonic signal and the surface appearance can be seen in Fig. 7. The as-polished cross section through the weld overlap region contains a planar defect parallel to the surface and has more than the usual amount of distributed porosity. It may be that these defects, particularly the planar one, reflect the ultrasonic signal as does a larger weld crack. Etching the weld overlap region revealed a normal grain structure (Fig. 8). The microstructure of the single-pass weld region was also normal, with many small grains along the centerline (Fig. 9).

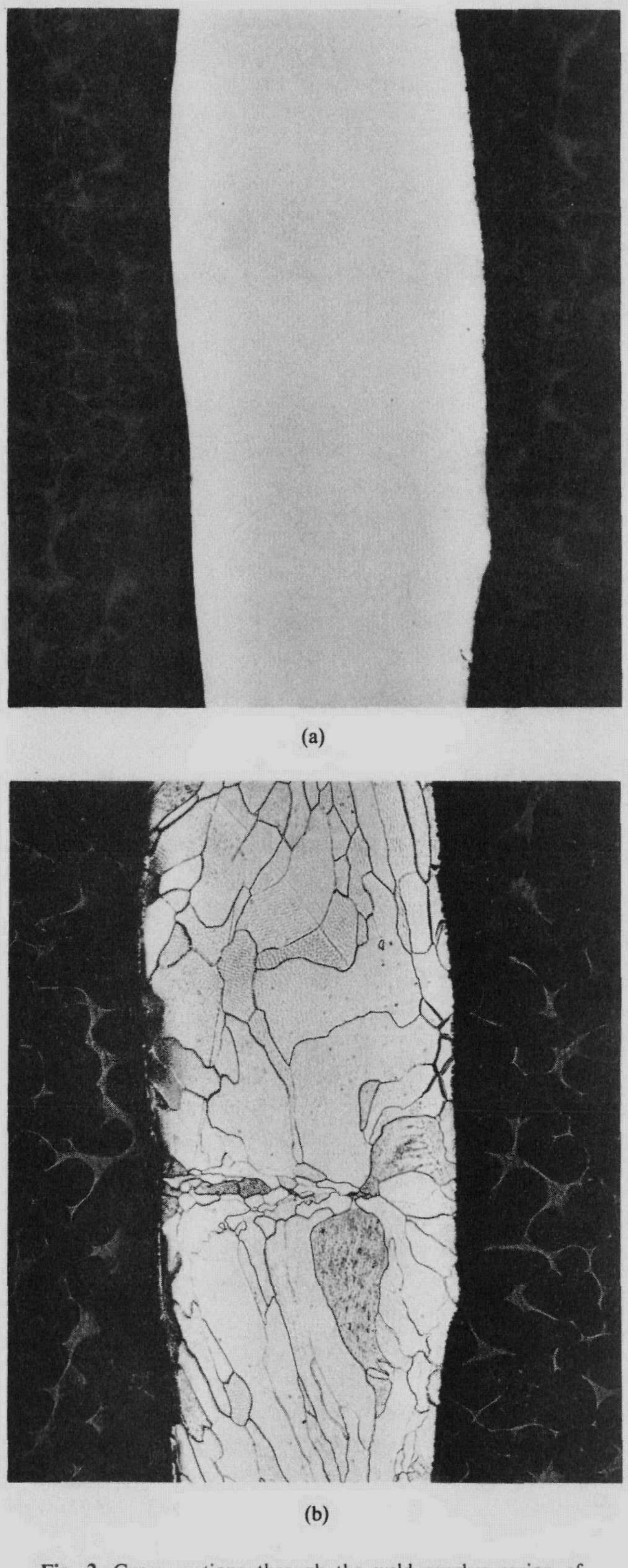

(a)

(b)

Fig. 2. Cross sections through the weld overlap region of capsule SRP-127 revealed only small surface cracks and a very small amount of grain-boundary porosity. (a) As-polished. (b) Etched. (50X)

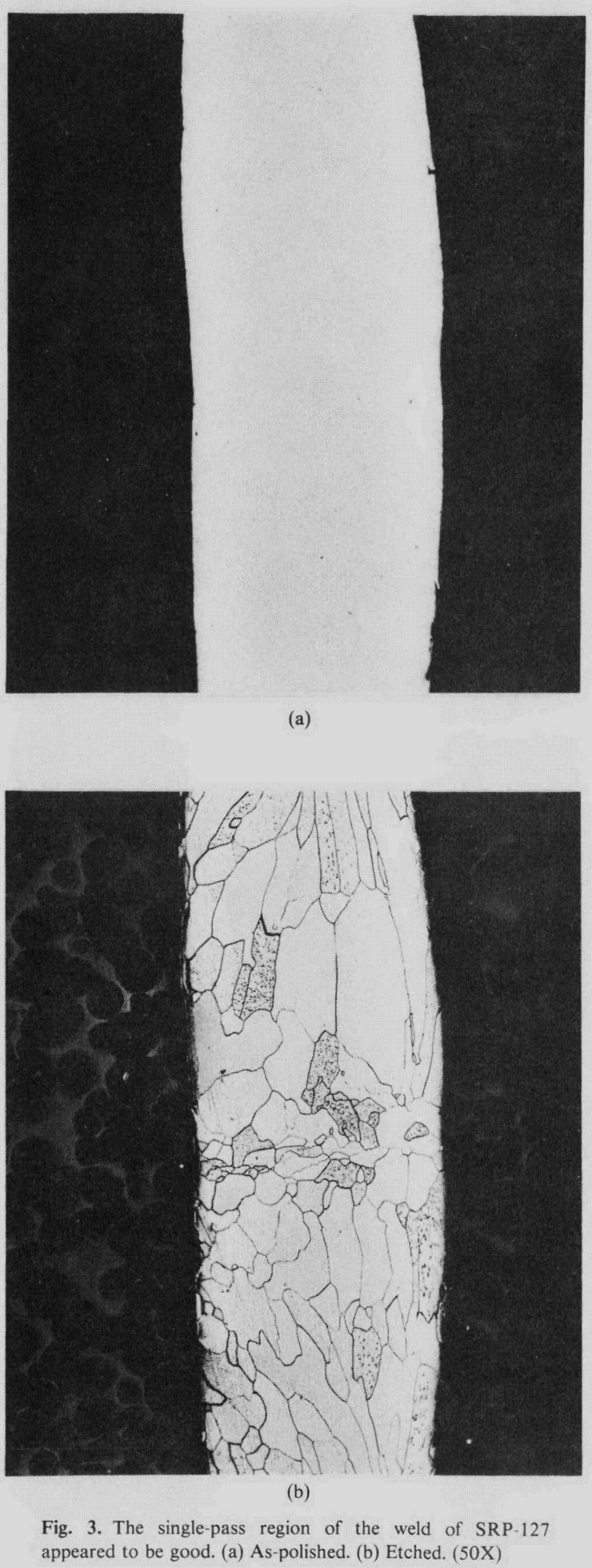

(a)

(b)

Fig. 3. The single-pass region of the weld of SRP-127 appeared to be good. (a) As-polished. (b) Etched. (50X)

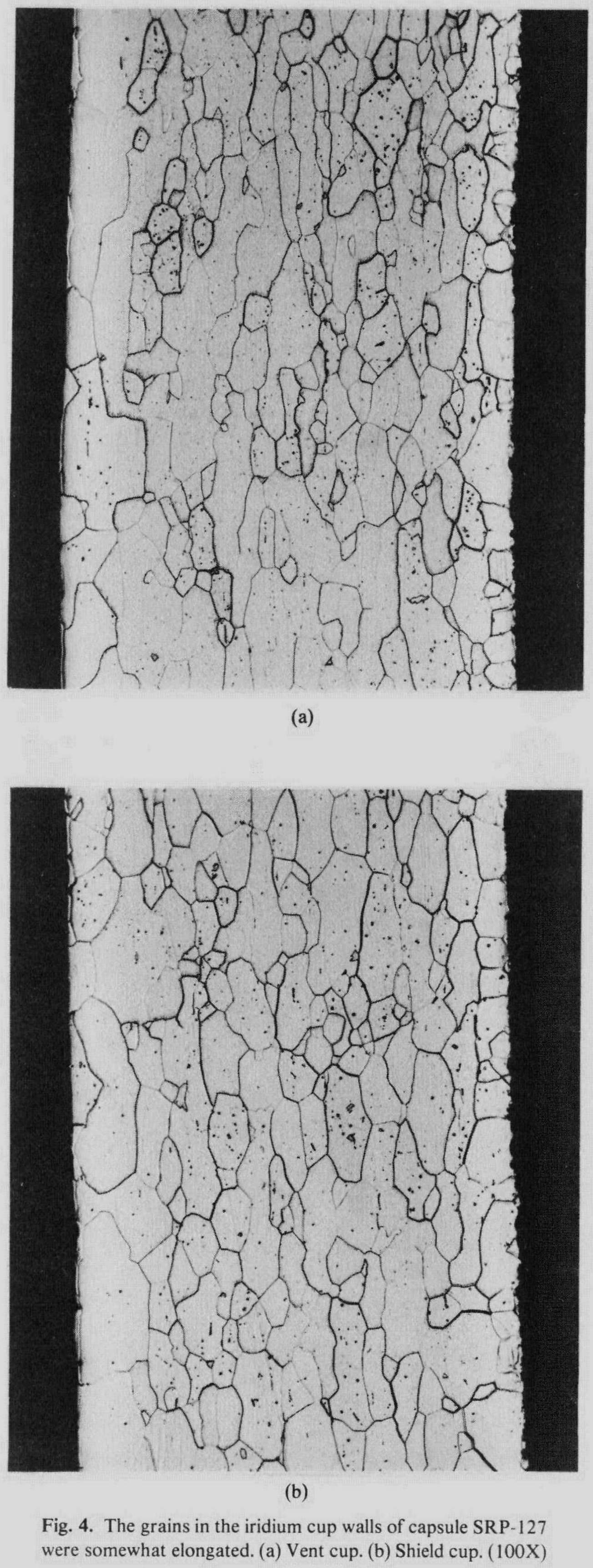

(a)

(b)

Fig. 4. The grains in the iridium cup walls of capsule SRP-127 were somewhat elongated. (a) Vent cup. (b) Shield cup. (100X)

Capsule No.	Cup Type	Grains/Thickness[a]
SRP-127	vent	21.5
	shield	18.1
SRP-140	vent	17.7
	shield	16.2
SRP-251	vent	16.4
	shield	17.4
SRP-317	vent	14.0
	shield	17.8

TABLE I. Transverse Grain Counts of the Iridium Capsules Used in the DIT-3 Impact

[a]In standard 640-μm thickness; average of five sections.

Fig. 6. Several fine cracks were visible in the weld overlap region just beyond the weld submergence in capsule SRP-140 (12X).

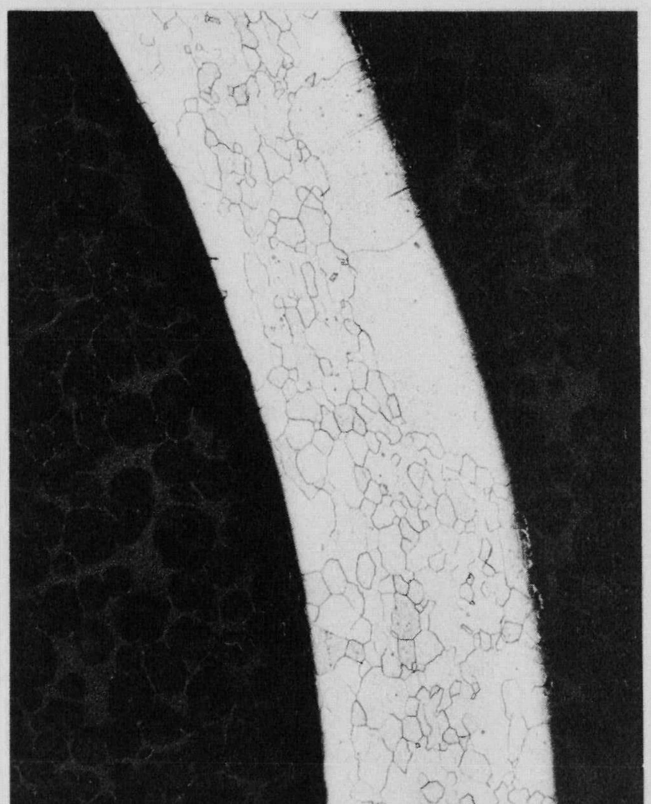

Fig. 5. Two very large grains were found on the outside of the radius of the vent cup from capsule SRP-127 (100X).

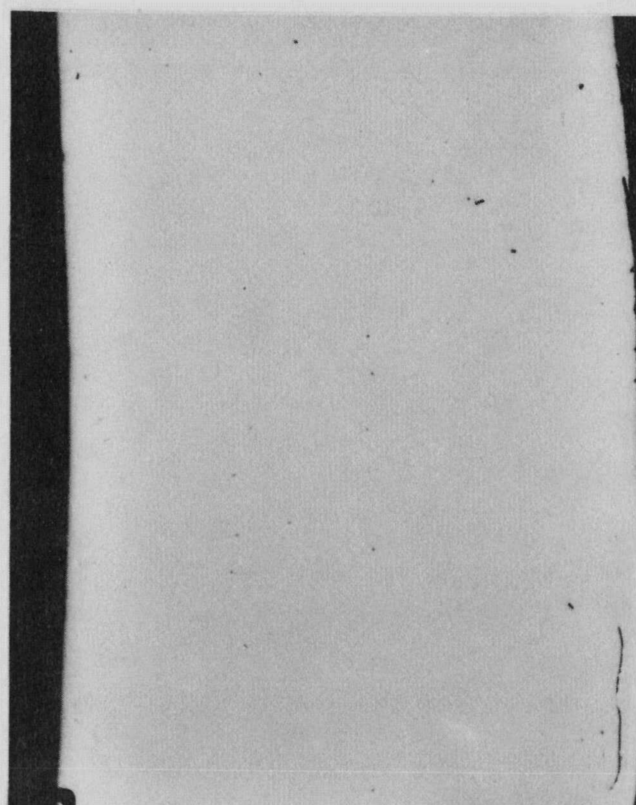

Fig. 7. The weld overlap region of capsule SRP-140 contained both a planar defect and distributed porosity (100X).

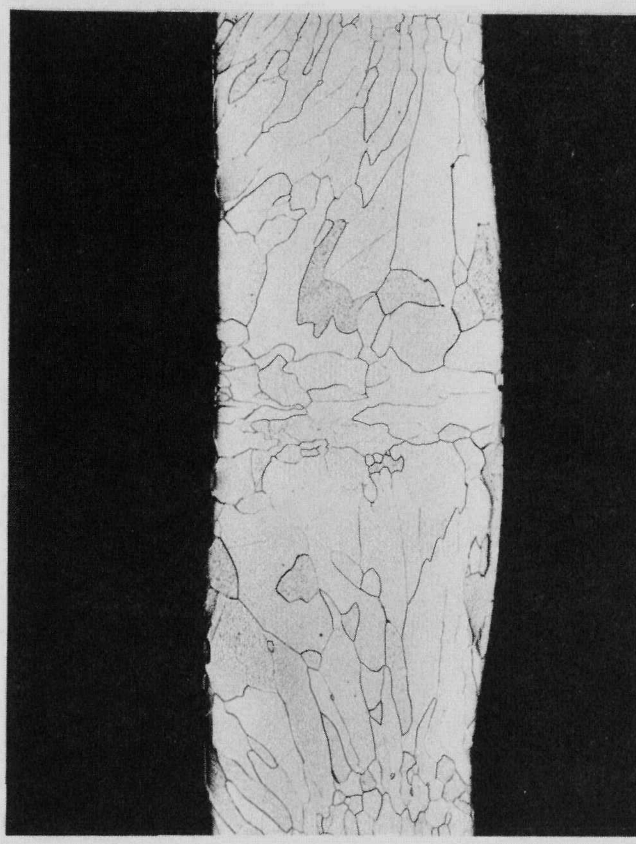

Fig. 8. The weld overlap region of capsule SRP-140 had a normal microstructure (50X).

Fig. 9. The single-pass weld in capsule SRP-140 was normal (50X).

Typical microstructures of the cup walls in capsule SRP-140 are shown in Fig. 10. The grains are not equiaxed in either cup. The average grain counts are listed in Table I.

3. Fueled Clad SRP-251. This fueled clad was in the leading position of impact assembly TGL-2, so it was in the closure end of the impact shell and faced an unpenetrated position of the reentry shell. Figure 11 shows that the internal surface in the weld overlap region appears rough and unreflective. The cross section through the region (Fig. 12) revealed a crack larger than the observed ultrasonic indication of 8.0 would suggest. Of course, the impact may have opened the crack and made it larger than it was at the time of the ultrasonic inspection.

The single-pass weld was normal (Fig. 13) and contained little porosity. There were many small grains along the weld centerline and no grain-boundary path straight through them.

Typical microstructures of the cup walls in capsule SRP-251 are shown in Fig. 14. The grain counts are listed in Table I.

4. Fueled Clad SRP-317. This fueled clad was in the leading position of impact assembly TGL-11, in the closed end of the impact shell facing a cap in the reentry shell. It had an ultrasonic indication of 10.4. The internal surface of the capsule in the weld overlap region is shown in Fig. 15. A classically typical weld crack is visible just beyond the point of weld submergence. This crack and the smaller ones are visible in the cross section through this region (Fig. 16).

The microstructure of the single-pass weld region of capsule SRP-317 was normal (Fig. 17), but there was some thinning at the edge of the weld pool. The typical microstructures of the cup walls (Fig. 18) show that the grains were elongated and that the vent cup (Fig. 18a) had grains larger than those in any other cup used in DIT-3. The measured grain counts are listed in Table I.

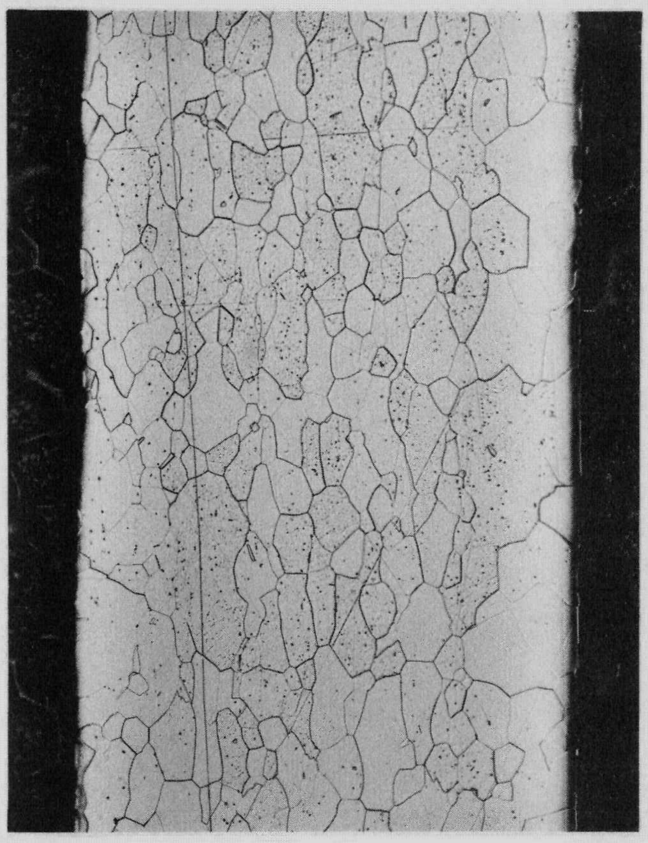

(a)

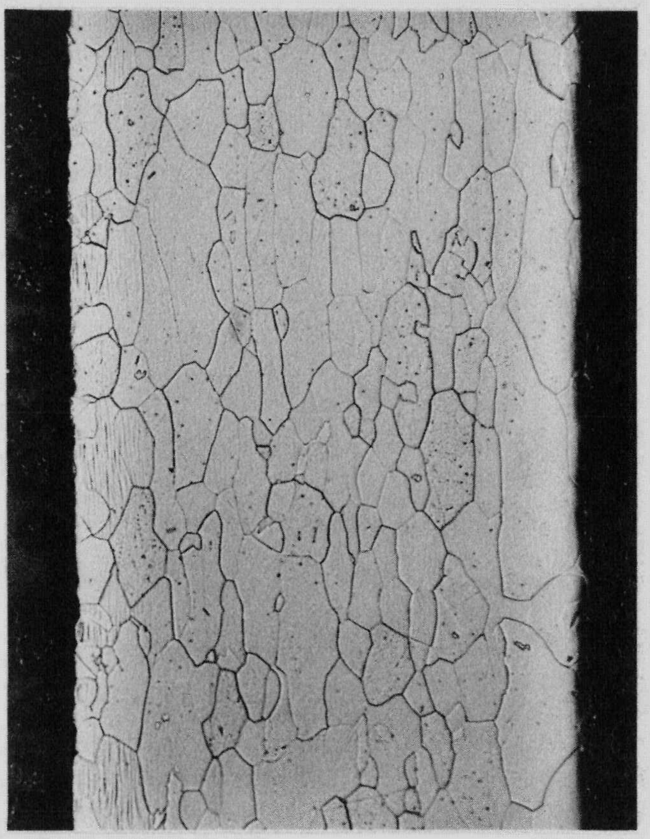

(b)

Fig. 10. The grains in capsule SRP-140 were somewhat elongated. (a) Vent cup. (b) Shield cup. (100X)

Fig. 11. The internal surface of the weld overlap region of capsule SRP-251 was rough and unreflective (12X).

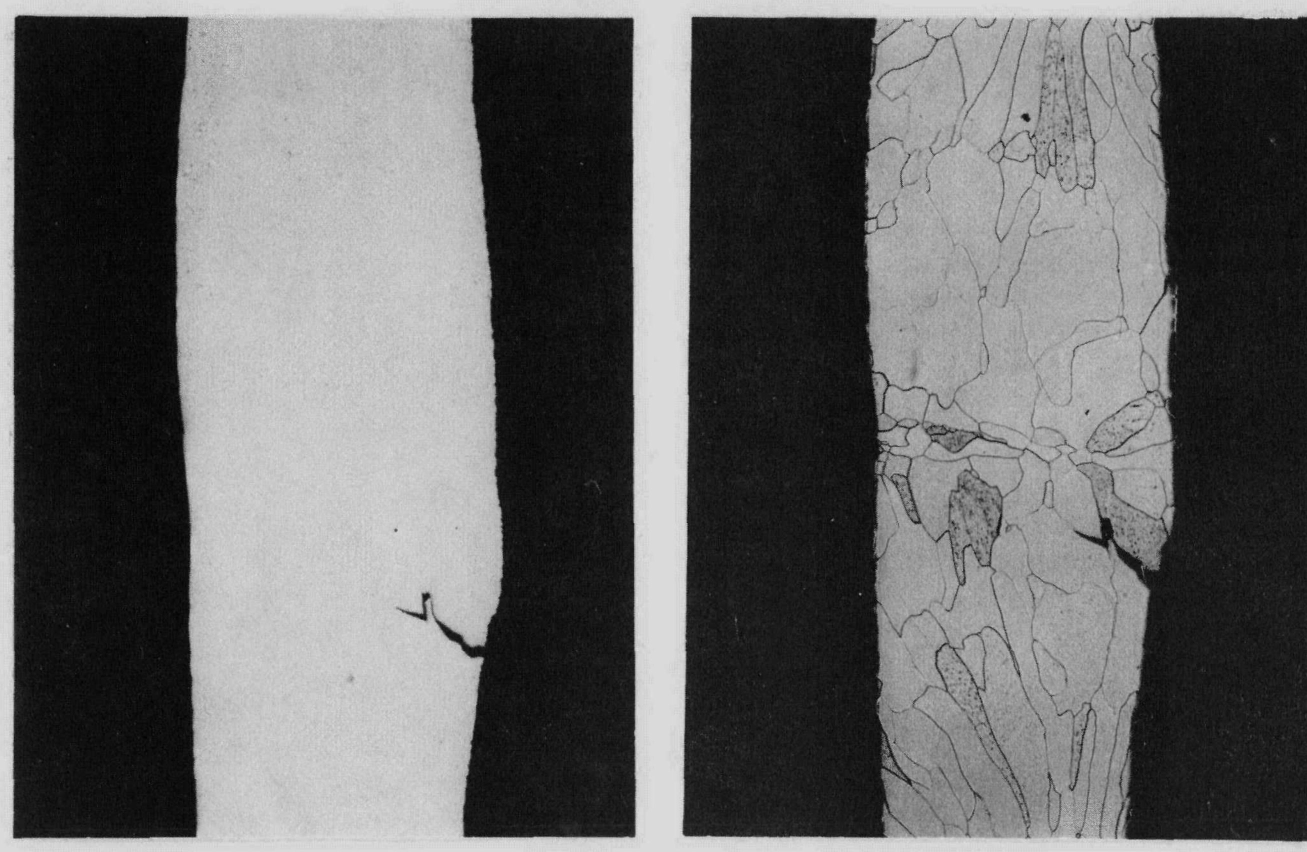

(a) (b)

Fig. 12. The weld overlap region of capsule SRP-251 contained a large crack but only limited porosity. (a) As-polished. (b) Etched. (50X)

Examination of the capsules used in DIT-3 revealed no cracks other than those in the weld overlap regions that presumably were present before the impact and caused the ultrasonic indications. The impact test results for all four capsules suggest that the 30° impact orientation used here is less severe than the 0° orientation used in the previous tests.

5. **DIT-3 Self-Heating (C. Frantz, R. Zocher).** The temperatures of a fuel clad in each impact assembly in the DIT-3 module are shown in Fig. 19. The clads, which were closely similar in temperature throughout the heating, took 86 min to reach the desired 930°C impact temperature. The DIT-3 temperature trace falls between the one for DIT-1 and those for DIT-2.[2] The prior samples took ~135 min and 64 min, respectively, to reach the impact temperature.

B. Future Impact Tests (R. Zocher)

In the fourth design iteration test (DIT-4), a partial module with a single impact assembly will be impacted in the 0° orientation after a 30-day aging treatment. The purpose of the test is to determine if iridium cups from which surface defects have been removed by mechanical polishing have a response to impact which is different from that of cups whose defects were polished out by hand. The aging treatment has been started.

A fifth design iteration test (DIT-5) is in the planning stages. Its purpose is to determine if there is a difference in impact response between fueled clads welded with two-pole and four-pole weld oscillators. The test will employ a partial module of the same design as that in DIT-4. The single impact assembly will contain one fueled clad welded with the two-pole oscillator and a second fueled clad welded with the four-pole oscillator.

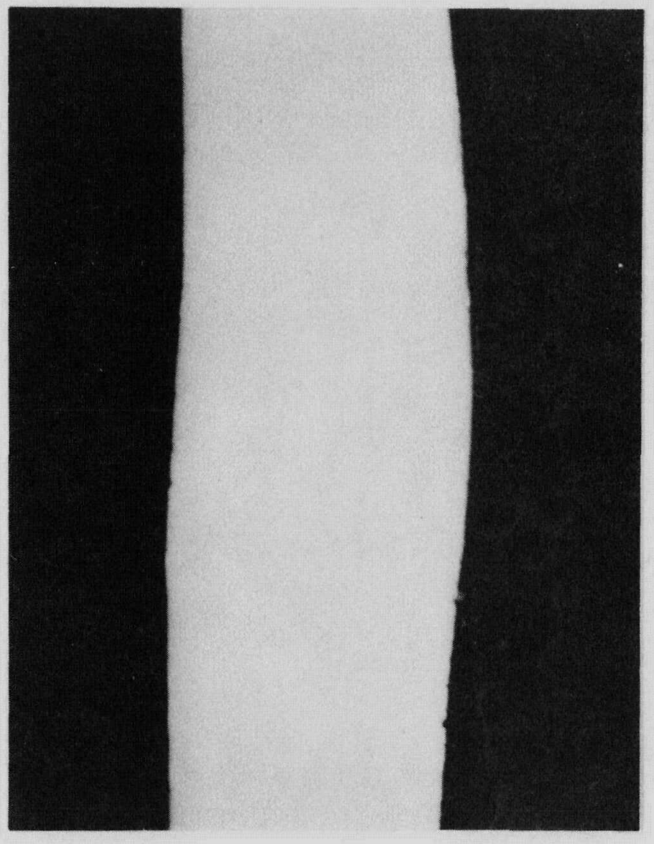

(a)

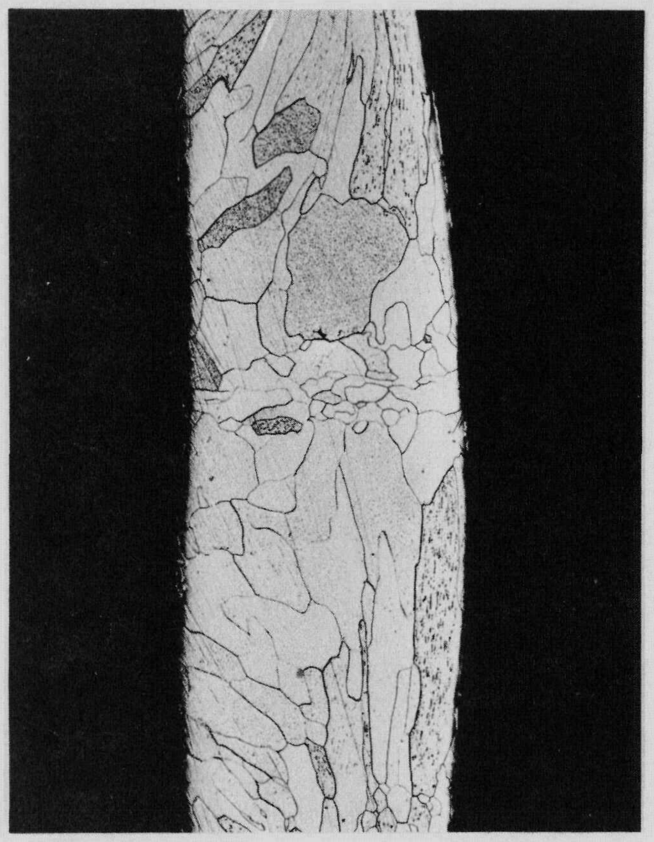

(b)

Fig. 13. The single-pass weld region in capsule SRP-251 was normal. (a) As-polished. (b) Etched. (50X)

C. Early Compatibility Test (D. Pavone)

The scheduled 6-month aging of this test assembly was completed on August 24, 1982. Continuous measurement of the helium release from the two fueled clads indicated that both vents remained open during August. The vent performance observations during the 6-month test exposure showed two periods of 41 and 66 h, respectively, during which the helium release was about half of the generation rate, suggesting that one of the vents was plugged. In contrast to the Multi-hundred Watt experience, periodic venting of helium by rapidly recurring bursts was not observed in this test.

D. Phosphorus Effects Experiment (D. Pavone)

The accumulated furnace exposure times on September 1, 1982, were 1834 h for the fueled assemblies and 785 h for the archive-ring control samples. The aging period will last 6 months.

The results of Auger electron spectroscopy (AES) analysis of fracture surfaces of nine of the archive-ring control samples are presented in Table II. The 10th sample (P714-5) was lost in the apparatus because of the difficulties encountered in mounting it; a duplicate of P714-5 will be submitted later. The results show thorium segregation at about the level expected for the DOP-26 iridium alloy. Except for single observations of an oxygen peak and a boron or chlorine peak, no grain-boundary impurities were detected.

Table III presents the grain-size data for the 10 specimens, along with the average Th_{65}/Ir_{229} AES intensity ratios. The grain sizes observed range from about 20 grains/640-μm thickness to about 30 grains/640-μm thickness. Although the AES data for the specimen with the largest grain size are not yet available, the remaining data do not suggest a correlation of grain size and Th/Ir AES intensity ratio.

The shapes of the iridium grains of the samples, except for one sample (PR719-6), were similar, with the grains elongated in the longitudinal direction. Sample PR719-6

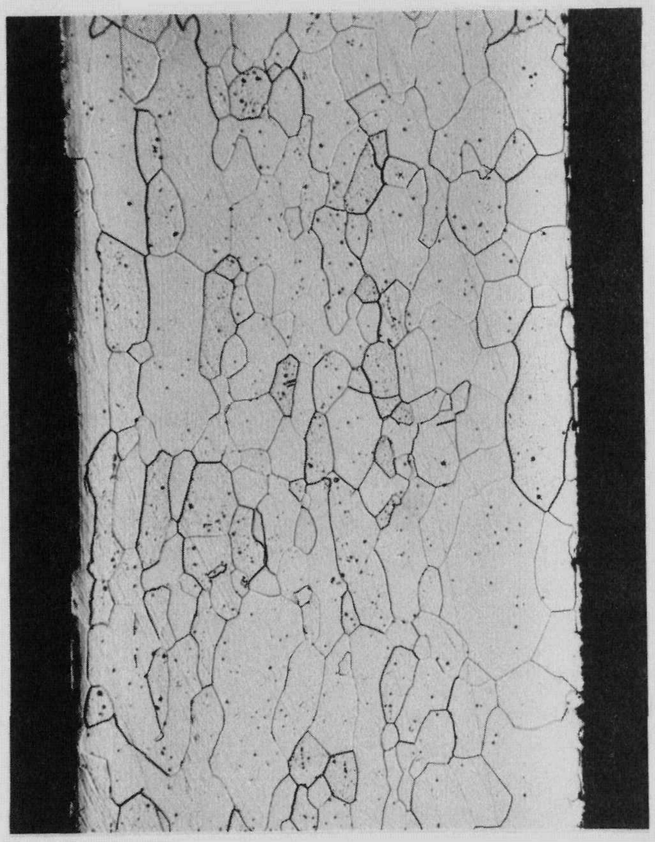

(a)

(b)

Fig. 14. The grains in both cups from capsule SRP-251 were slightly elongated. (a) Vent cup. (b) Shield cup. (100X)

Fig. 15. A classically typical weld crack is visible in the overlap region just beyond the point of weld submergence in capsule SRP-317 (12X).

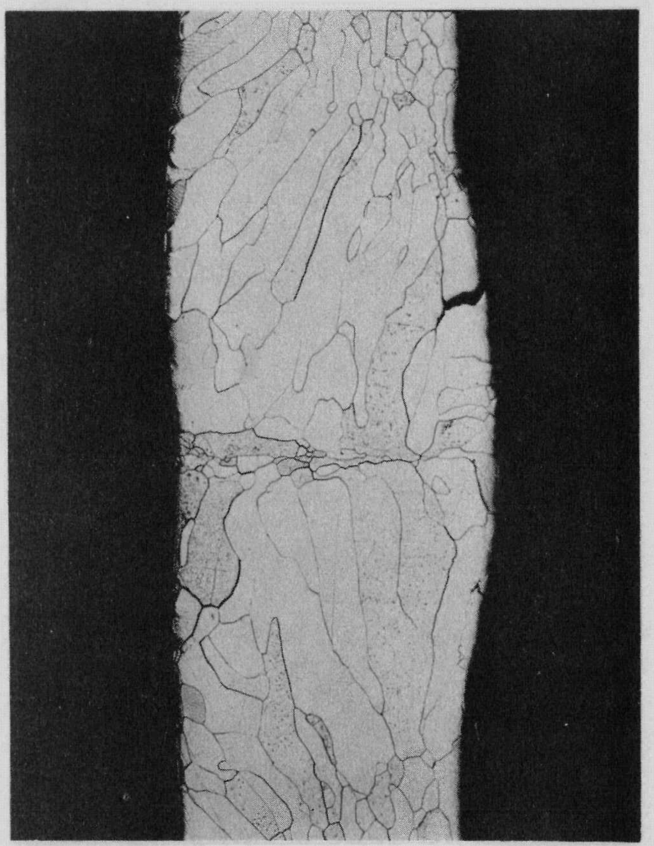

Fig. 16. The weld cracks are visible in this cross section of the weld overlap region of capsule SRP-317 (50X).

Fig. 17. The single-pass weld of capsule SRP-317 had a normal microstructure (50X).

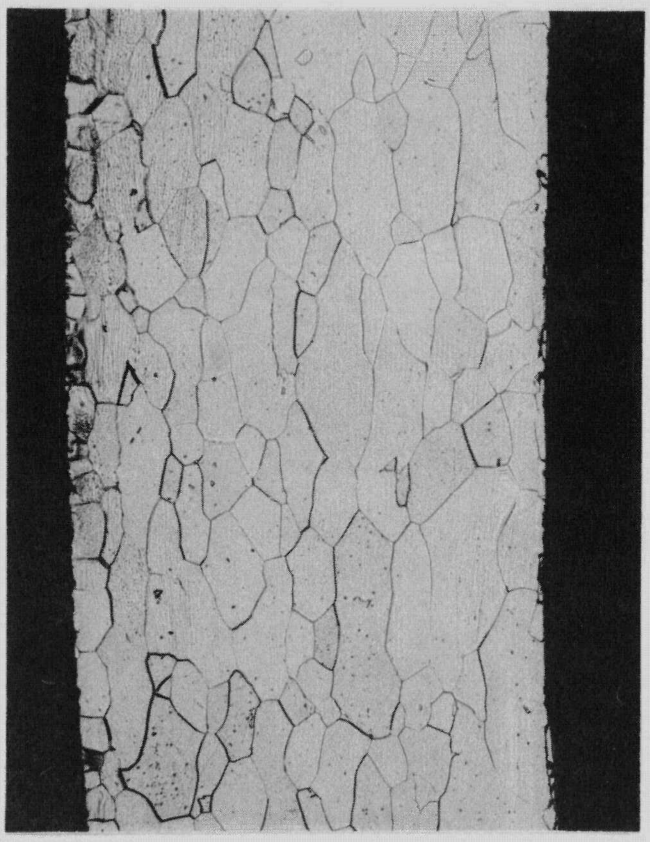

(a)

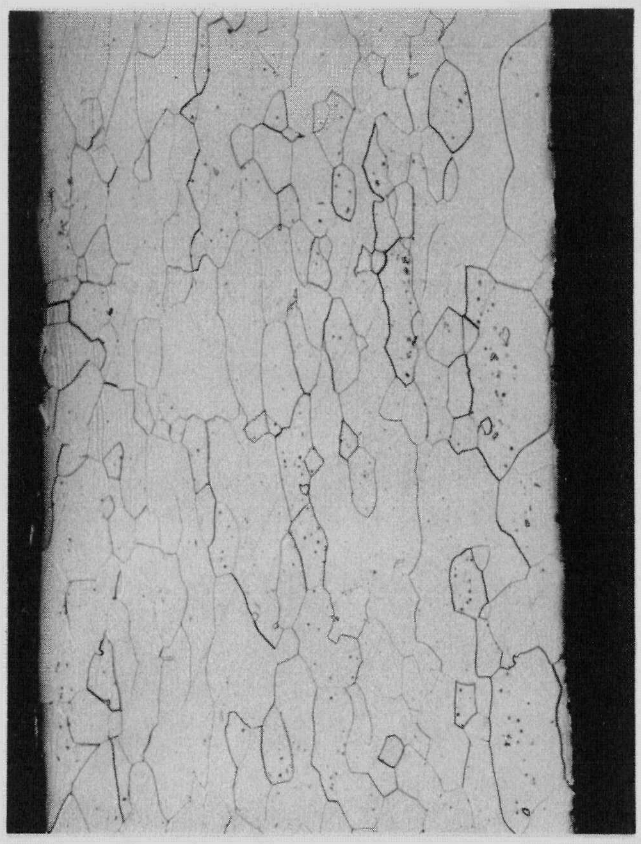

(b)

Fig. 18. The grains in both cups that made up capsule SRP-317 were elongated. Those in the vent cup were larger than those in any other cup used in DIT-3. (a) Vent cup. (b) Shield cup. (100X)

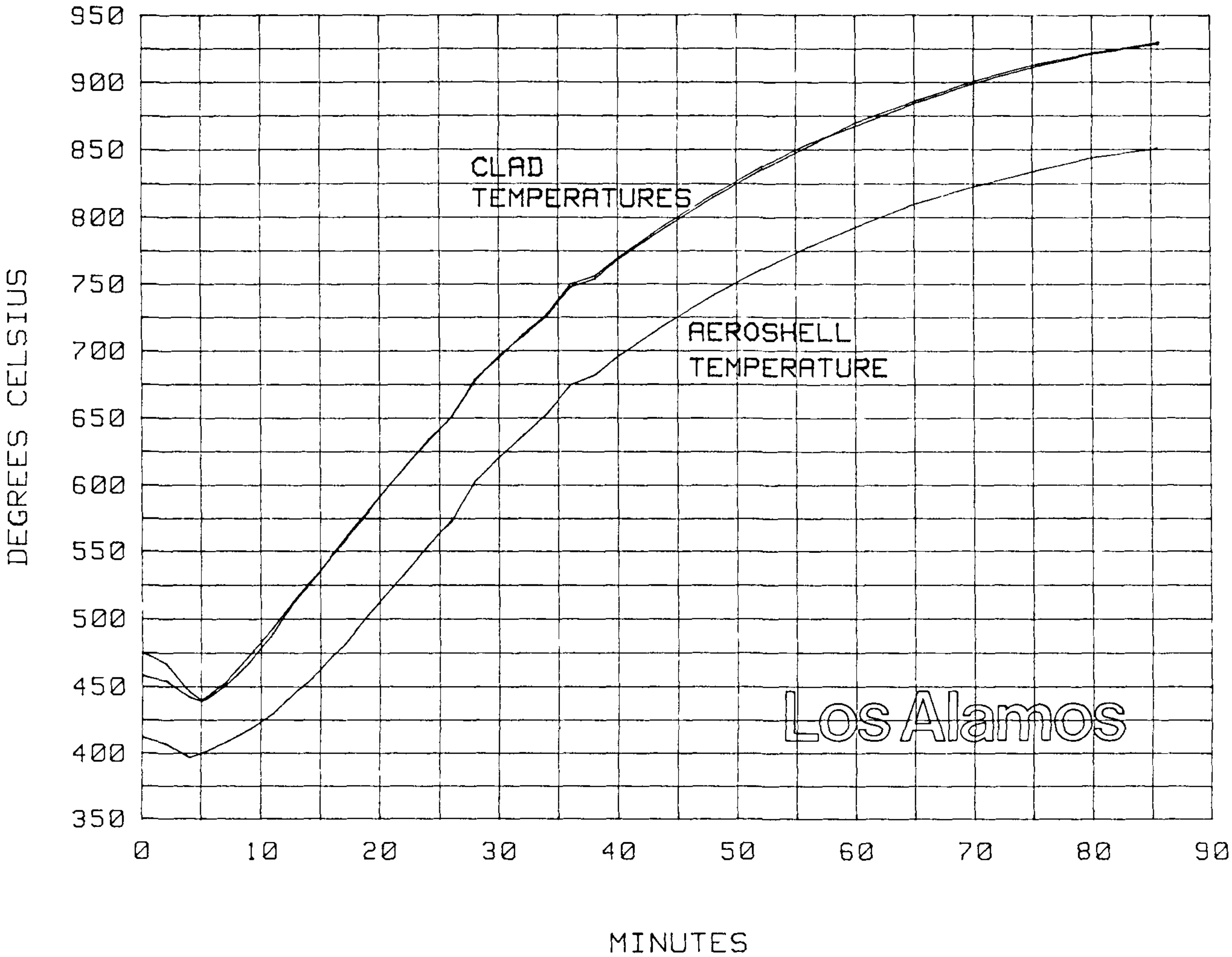

Fig. 19. Both instrumented clads in the DIT-3 test had the same self-heating thermal history before impact.

TABLE II. AES Intensity Ratios for GPHS Archive Rings

Cup No.	Location	Th_{65}/Ir_{229}	Th_{65}/Ir_{54}	Other
L254-7	Inside	0.78	0.08	
	Center	0.88	0.08	
	Outside	0.70	0.07	
	Average	0.79	0.08	
L256-8	Inside	0.80(?)	0.07	
	Center	0.66	0.07	
	Outside	0.80	0.08	
	Average	0.75	0.07	
L255-6	Inside	0.80	0.07	
	Center	0.96	0.10	
	Outside	0.87	0.08	
	Average	0.88	0.09	
L257-R2	Inside	0.82	0.08	
	Center	1.08	0.11	
	Outside	0.55	0.06	
	Average	0.82	0.08	
P701-4	Inside	0.57	0.07	
	Center	0.84	0.09	
	Outside	0.75	0.08	
	Average	0.78	0.08	
N502-3	Inside	0.60	0.06	0.15 B or Cl_{180}/Ir_{22}
	Center	0.91	0.09	
	Outside	0.64	0.07	
	Average	0.72	0.07	
PR715-2	Inside	0.74	0.07	
	Center	0.84	0.08	
	Outside	0.66	0.08	
	Average	0.75	0.08	
PR719-6	Inside	0.91	0.09	
	Center	0.94	0.09	
	Outside	0.65	0.07	0.56 O_{510}/Ir_{229}
	Average	0.83	0.08	
NR520-2	Inside	0.89	0.09	
	Center	0.78	0.08	
	Outside	0.71	0.08	
	Average	0.79	0.08	
P714-5[a]				

[a]Not yet analyzed.

TABLE III. Grain Size of Ir-0.3W Archive Rings[a]				
Cup No.	Section Thickness (μm)	Grains/ Thickness	Grains/ 640-μm Thickness	Th_{65}/Ir_{229} AES Ratio
L254-7	680	31.3	29.5	0.79
L256-8	673	27.5	26.2	0.75
L255-6	700	27.3	25.0	0.88
L257-R2	667	31.6	30.3	0.82
P701-4	687	24.7	23.0	0.78
N502-3	642	25.2	25.1	0.72
PR715-2	647	27.2	26.9	0.75
PR719-6	700	26.4	24.1	0.83
NR520-2	677	27.1	25.6	0.79
P714-5	680	21.5	20.2	[b]

[a]Annealed 1 h at 1500°C.
[b]Not yet analyzed.

exhibited a more nearly equiaxed grain shape. Figure 20 illustrates the range of grain sizes observed in these samples and the contrasting grain shape of sample PR719-6.

II. LIGHT-WEIGHT RADIOISOTOPE HEATER UNIT (R. Tate)

The preliminary documentation for the Light-Weight Radioisotope Heater Unit production parts was reviewed. Forty-one items were accepted as prime-quality hardware suitable for flight use.

ERRATA

In reference to deposits in the iridium filter element in MHW-FSA MHFT-76 described in the last paragraph on page 9 and continued on page 12 of the May report (LA-9547-PR):[3]

The word "metallic" should be "nonmetallic" and the element "cerium" should be "chromium."

REFERENCES

1. S. E. Bronisz (Comp.), "Flight Systems Safety Program, July 1982," Los Alamos National Laboratory report LA-9550-PR (October 1982).

2. S. E. Bronisz (Comp.), "Space Nuclear Safety and Fuels Program, October 1981," Los Alamos National Laboratory report LA-9280-PR (March 1982).

3. S. E. Bronisz (Comp.), "Flight Systems Safety Program, May 1982," Los Alamos National Laboratory report LA-9547-PR (October 1982).

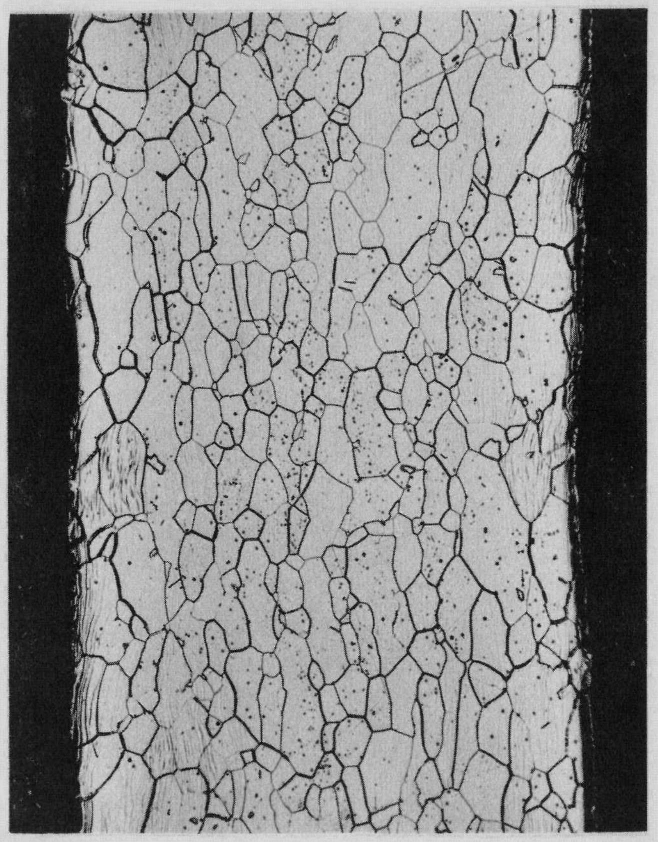

(a)

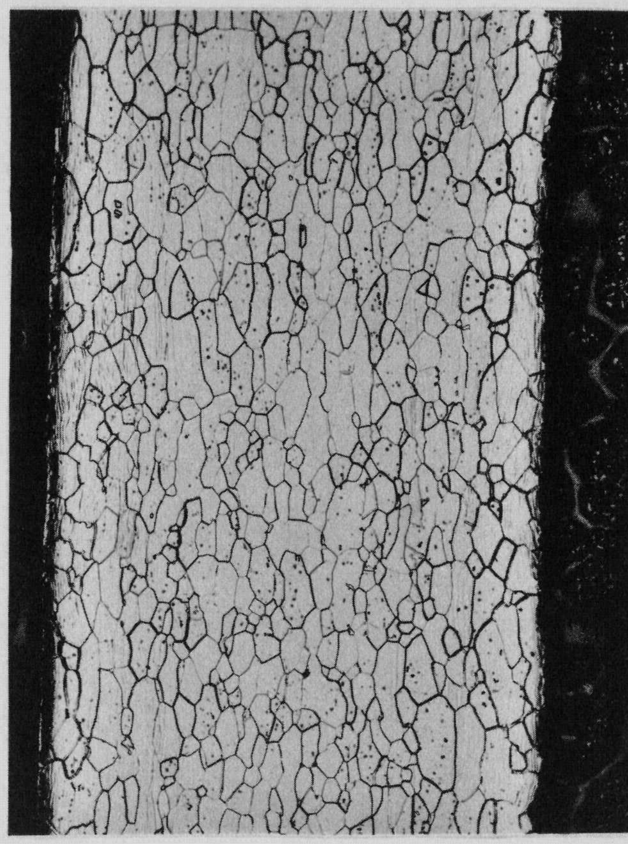

(b)

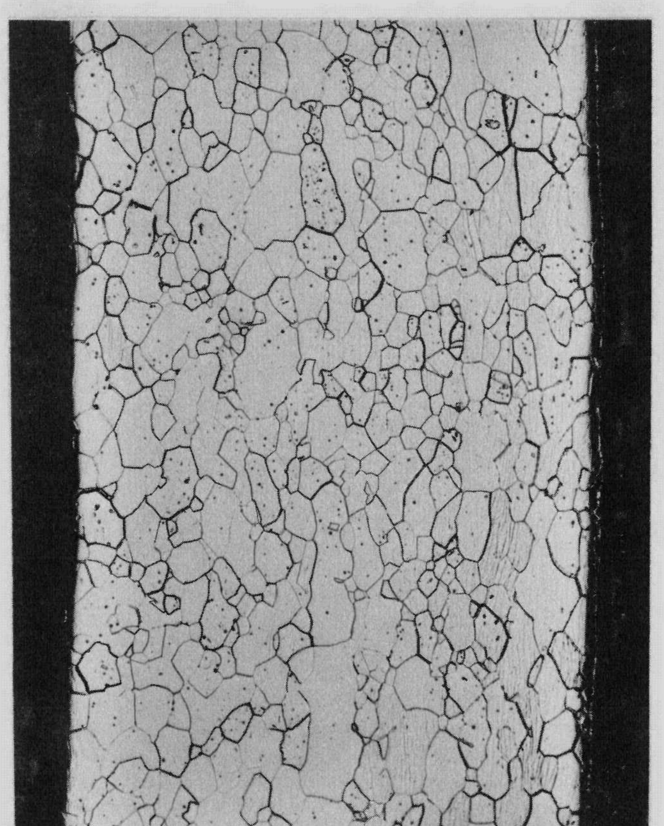

(c)

Fig. 20. The grains in the archive rings from the iridium cups used in the phosphorus effects experiment were generally elongated. (a) P714-5, 20.2 grains/640-μm thickness, the coarsest grained sample. (b) L257-R2, 30.3 grains/640-μm thickness, the finest grained sample. (c) PR719-6, 24.1 grains/640-μm thickness, the only equiaxed sample. (100X)

DO NOT MICROFILM

ADDITIONAL DISTRIBUTION

B. J. Rock, Dept. of Energy/OSNP, Washington, DC
G. L. Bennett, Dept. of Energy/OSNP, Washington, DC
J. J Lombardo, Dept. of Energy/OSNP, Washington, DC
R. B. Morrow, Dept. of Energy/OSNP, Washington, DC
R. Brouns, Dept. of Energy/OSNP, Washington, DC
C. O. Tarr, Dept of Energy/OSNP, Washington, DC
J. Griffo, Dept. of Energy/OSNP, Washington, DC
D. K. Stevens, Dept. of Energy/BES, Washington, DC
M. Norin, Dept. of Energy, Washington, DC
G. Ogburn, Dept of Energy, Washington, DC
J. A. Yoder, Dept. of Energy, Washington, DC
C. Osterberg, Dept of Energy, Washington, DC
I Van Der Hoven, Dept. of Energy, Washington, DC
R. L. Clark, Dept. of Energy/ALO, Albuquerque, NM
J. P. Crane, Dept of Energy, Albuquerque, NM
K Elliot, Dept. of Energy, Albuquerque, NM
D. L. Krenz, Dept. of Energy, Albuquerque, NM
J. R. Roeder, Dept of Energy, Albuquerque, NM
R. B. Crouch, Dept. of Energy, Albuquerque, NM
J. N. Bailey, Dept. of Energy, Albuquerque, NM
H. N Hill, Dept. of Energy/DOA, Miamisburg, OH
L. C. Sjostrom, Dept. of Energy, Aiken, SC
R. J. Hart, Dept. of Energy/ORO, Oak Ridge, TN
J. Pidkowicz, Dept of Energy, Oak Ridge, TN
W L. Von Flue, Dept of Energy, SFOO, Oakland, CA
T B Kerr, NASA, Washington, DC
F. R. Schmidt, NASA, Washington, DC
E. Gabris, NASA, Washington, DC
N. Sculze, NASA, Washington, DC
B. R McCullar, NASA, Washington, DC
Operations and Systems Requirements, NASA, Washington, DC
A. V. Diaz, NASA, Washington, DC
R. G. Ivanoff, NASA/JPL, Pasadena, CA
R. Campbell, NASA/JPL, Pasadena, CA
L. T. Shaw, JPL, Pasadena, CA
R. J Spehalski, JPL, Pasadena, CA
AFISC/SNS, Attn Col J A Richardson, Kirtland AFB, NM
AFISC/SNS, Attn Maj John Rice, Kirtland AFB, NM
AFWL/NTYVS, Attn· Capt J D Martens, Kirtland AFB, NM
Lt. Col. James H. Lee, AFWL/NTED, Kirtland AFB, NM
Lt. Michael K Seaton, AFWL/NTED, Kirtland AFB, NM
Maj. Ray Baca, HQ AFSC/IGF, Andrews AFB, Washington, DC
Col. William Licht, ATSD/AE, Washington, DC
Lt. John Erb, ESMC/SGPH, Patrick AFB, FL
L. J. Ullian, ESMC/SE, Patrick AFB, FL
Dr. W Keesler, AFML/MPE, Wright Patterson AFB, OH
Lt. Douglas Zimmerman, AFWL/NTYVS, Kirtland AFB, NM
Lt. Col Mel Nosal, AFISC/SES, Norton AFB, CA
Lt. Col. Ken Morrison, AFISC/SES, Norton AFB, CA
Maj. Walt Wilson, AFISC/SEM, Norton AFB, CA
John Marshall, AFRPL/LKC, Edwards AFB, CA
Lt. Col. William B Moyer, AFMSC/SGPZ, Brooks AFB, TX
W. Riley, WSMC/SE, Vandenberg AFB, CA
Capt. Charles Snow, SAMSO/SE, Los Angeles, CA
HQ Space Div./YLVS, Attn. Lt. Col. Needham, Los Angeles, CA
R. L. Folger, SRL, Aiken, SC
J. Howell, SRL, Aiken, SC
J. B. Mellen, SRP, Aiken, SC
D. Nichols, SRP, Aiken, SC
D. Bickford, SRP, Aiken, SC
J R. McClain, MRC, Miamisburg, OH
W. T. Cave, MRC, Miamisburg, OH
W. Amos, MRC, Miamisburg, OH
E. W. Johnson, MRC, Miamisburg, OH
R. Cooper, ORNL, Oak Ridge, TN
C. Alexander, BCL, Columbus, OH
E E Rice, BCL, Columbus, OH
J. Hagan, APL, Baltimore, MD
B. Bartram, NUS Corporation, Gaithersburg, MD
R. W. Englehart, NUS Corporation, Gaithersburg, MD
H. H Van Tuyl, PNL, Richland, WA
A. Schock, Fairchild Hiller Ind., Germantown, MD
E. Skrabek, Fairchild-Hiller Ind., Germantown, MD
C W Whitmore, GE, Philadelphia, PA
C. T Bradshaw, GE, Philadelphia, PA
R. Kelley, GE, Philadelphia, PA
R. Hemler, GE, Philadelphia, PA
V. Haley, GE, Philadelphia, PA
R. Hartman, GE, Philadelphia, PA
W. Mecham, ANL, Argonne, IL
D C Anderson, Teledyne Energy Systems, Timonium, MD
P. Dick, Teledyne Energy Systems, Timonium, MD
Dr. Marvin Goldman, University of California, Davis, CA
Charles Smith, Sandia National Laboratories, Albuquerque, NM
R. Harner, Sandia National Laboratories, Albuquerque, NM
J. Calek, Sandia National Laboratories, Albuquerque, NM
C. M. Barnes, L. B Johnson Space Center, NASA SPS, Houston, TX
R H Brown, L B Johnson Space Center, NASA FM, Houston, TX
R. G Rose, L. B. Johnson Space Center, NASA FA, Houston, TX
Harold Battaglia, L. B Johnson Space Center, NASA PF, Houston, TX
W. H Boggs, NASA, DE-A, J. F Kennedy Space Center, FL
Lloyd Parker, NASA, SF, J F. Kennedy Space Center, FL
George M. Marmaro, NASA, MD-ESB, J. F Kennedy Space Center, FL
W A Riehl, Marshall Space Flight Center, NASA, EH31, Marshall SFC, AL
W. C Pitts, NASA, STPM, Ames Research Center, Moffett Field, CA
J J Givens, Ames Research Center, Moffett Field, CA
R Corridan, Ames Research Center NASA, Moffett Field, CA
J C. Robinson, Langley Research Center, NASA, MS395, Hampton, VA
G J. Schaefer, Jr , Lewis Research Center, NASA, MAIC 500-120, Cleveland, OH
R. C. Turkolu, TRW, Defense and Space Systems Group, Redondo Beach, CA
D Eaton, European Space Research and Technology Centre, Zwarteweg 62, Njordwijk, The Netherlands
Dr. Ralph R. Fullwood, Science Applications, Inc., Palo Alto, CA
Dr William Ailor, The Aerospace Corporation, Los Angeles CA
T. Carter, Nuclear Regulatory Commission, Washington, DC
C. R. Chappell, Nuclear Regulatory Commission, Washington, DC
D. Egan, Office of Radiation Programs, USEPA, Washington, DC
N Elsner, General Atomics, San Diego, CA
Charles Salisbury, Naval Ocean Systems Center, San Diego, CA
Dr Herbert Weiss, Naval Ocean Systems Center, San Diego, CA
W J Maraman, Los Alamos National Laboratory, Los Alamos, NM
S. S. Hecker, Los Alamos National Laboratory, Los Alamos, NM
R. N. R. Mulford, Los Alamos National Laboratory, Los Alamos, NM
J. Birely, Los Alamos National Laboratory, Los Alamos, NM
W. F Miller, Los Alamos National Laboratory, Los Alamos, NM
R. J Pryor, Los Alamos National Laboratory, Los Alamos, NM
S E. Bronisz, Los Alamos National Laboratory, Los Alamos, NM
W. Stark, Los Alamos National Laboratory, Los Alamos, NM
R. W. Zocher, Los Alamos National Laboratory, Los Alamos, NM
J. A Pattillo, Los Alamos National Laboratory, Los Alamos, NM
E. M Wewerka, Los Alamos National Laboratory, Los Alamos, NM